

Dependence of the linewidth of planar electron channeling radiation on the thickness of the diamond crystal

B. Azadegan,* W. Wagner,[†] and J. Pawelke

Forschungszentrum Rossendorf, Institute of Nuclear and Hadron Physics, D-01314 Dresden, Germany

(Received 6 February 2006; revised manuscript received 28 April 2006; published 17 July 2006)

Measurements of (110) planar channeling radiation have been performed at the radiation source ELBE at electron energies of 14.6, 17, 30, and 34 MeV using diamond crystals of thickness 42.5, 102, 168, and 500 μm . The influence of different line-broadening mechanisms on the spectral shape of radiation from the 1–0 transition has been investigated. The analysis bases on fitting a convolution of the intrinsic Lorentz-like line shape with a Gaussian-like multiple-scattering distribution to the measured spectra. The asymmetry parameter involved relates to the standard deviation of the effective multiple-scattering angle. Its dependence on the crystal thickness was found to be weaker than for nonchanneled particles. The deduced coherence lengths show no significant dependence on the electron energy.

DOI: 10.1103/PhysRevB.74.045209

PACS number(s): 61.85.+p

I. INTRODUCTION

Channeling radiation (CR) is a well known phenomenon since the middle of the 1970s.^{1–4} It is emitted by relativistic charged particles during their interaction with the averaged periodic field generated by structures of high symmetry in single crystals such as axes and planes. To date the main characteristics of CR are adequately established. The physics of CR has been incorporated into textbooks, fills monographs, or can be studied from review articles, which mostly contain numerous references to the original works.^{5–10} The interest in CR was gained especially during the 1990s because of its proclaimed possible application as a rather intensive and easily tunable, quasimonochromatic source of x-rays at electron beams of even moderate energy (10–50 MeV).^{11–13} Some modern precondition for subsequent systematic and application oriented studies of CR was provided by the construction and availability of relatively compact superconducting electron accelerators which are able to deliver intense electron cw beams of low emittance.^{14,15}

For the purpose of this application, the optimization of the yield and spectral linewidth of CR became an issue of intensive investigations.^{16–26} Diamond crystals have been found to be probably the most suitable ones for intense CR production because of their outstanding parameters such as low atomic number, perfect structure, high Debye temperature, large thermal conductivity, etc.^{11,12} Unfortunately, most of the experimental investigations, which have been performed with diamond crystals up to now, were restricted either to relatively high^{16–19} or low energy.^{11,21–24} Furthermore, they typically concerned only relatively thin crystals. Some of the deduced systematics, therefore, appears to be incompletely verified on a quantitative scale.

The present work deals with the investigation of the influence of the thickness of the diamond crystal on the residual linewidth of CR and covers up to now inviolate but application relevant energy region between 14 and 34 MeV. Since in earlier works the 1–0 transition of (110) planar CR from diamond crystal has been explored as that of maximum yield,^{21–23} we just concentrated on this line only.

It must be pointed out that first attempts to investigate CR linewidths for diamond crystals have been undertaken in Refs. 17 and 18. Afterwards, measurements at electron energies of 5.2 and 9 MeV have been performed,^{21,23} but conclusions could cover only crystal thicknesses up to 55 μm . In a recent work,²⁴ a 204 μm thick diamond crystal was used but the linewidth has not been considered explicitly.

Rather comprehensive investigations with Si and Ge crystals were reported in Refs. 19 and 25. Some conclusions drawn in the above specified papers, however, differ from those made in Ref. 26 where partly the same experimental data are interpreted.

II. MEASUREMENTS

The measurements of^{27–29} CR used for the present analysis have been carried out at the electron beam of the radiation source ELBE¹⁵ at the Forschungszentrum Rossendorf. The linear electron accelerator ELBE is a superconducting rf machine, which actually covers the energy range from 10 to 35 MeV at a maximum average beam current of about 1 mA. It consists of a thermionic dc electron gun, an injector stage preaccelerating the electrons to 250 keV, two rf bunching sections forming micropulses of about 2 ps duration and four superconducting cavities operating at a frequency of 1.3 GHz. The pulse repetition rate can be set to 13, 26, and 260 MHz.

For channeling experiments the maximum available electron current is restricted to 100 μA . For the reason of appropriate detector counting rates, the average beam current in our measurements, however, amounted typically to several nanoamperes only. Beam collimation within the injector stage at low energy allows one to improve the emittance to values less than 3 mm mrad (rms) resulting in a beam divergence of nearly 0.1 mrad. The beam-energy spread amounts to 1.3×10^{-3} while energy tuning was possible to an accuracy of about 0.2–0.3 MeV.

All the diamond crystals used in our measurements are of type IIa and of [110] cut. The measured thicknesses amount to $(42.5 \pm 4.0) \mu\text{m}$, $(102.2 \pm 4.7) \mu\text{m}$, $(168.0 \pm 3.9) \mu\text{m}$, and $(500 \pm 25) \mu\text{m}$. A goniometer³⁰ assures the alignment of the

crystals to the channeling condition with an angular resolution of 0.5 mrad. After passing the crystal, the electron beam is deflected by means of a dipole magnet into the beam dump. The radiation has to penetrate a 127 μm thick Be-window separating the ultrahigh vacuum of the beam line, an auxiliary vacuum line evacuated to 1.5 mbar and 45 cm of air. These materials limit the lower registration threshold to about 5 keV.

A CdTe detector (AMPTTEK) has been applied for spectrometry of CR. The detector position at zero degree with respect to the beam axis and 3.3 m away from the crystal target has been checked to an accuracy of 0.1 mm. A massive Pb collimator with an aperture of only 1 mm shields the detector from background radiation and defines the solid angle of the measurement to 7.2×10^{-8} sr as well. Over the energy range of 10–70 keV the registration efficiency of the CdTe detector is nearly equal to one, and then it decreases with increasing energy. ^{241}Am , ^{55}Fe , ^{133}Ba , and ^{210}Pb sources have been applied for energy calibration. The FWHM of the 13.93 keV line of ^{241}Am amounted to (470 ± 2) eV. During the measurement time, the electron-beam current has been recorded by means of a very thin secondary emission monitor (SEM)^{31–33} positioned directly behind the crystal to prevent counting losses due to electron scattering in the target. The absolute current calibration of the SEM was carried out against an especially constructed Faraday cup moveable into and out of the electron beam.

III. THEORY

A. Preliminaries

When a relativistic charged particle passes through a single crystal parallel to some axis or plane it emits CR. At moderate energies (< 100 MeV) the emission of electromagnetic CR corresponds to a spontaneous transition of the channeled particle between two transverse eigenstates in the continuum potential of that axis or plane. The calculation of the eigenvalues and, consequently, of the CR transition energies, represents a many-beam problem.³⁴

In the case of planar electron channeling, the eigenstates can be computed by solving the one-dimensional quasi-Schrödinger equation

$$-\frac{\hbar^2}{2\gamma m_e} \frac{d^2\psi(x)}{dx^2} + V(x)\psi(x) = E\psi(x), \quad (1)$$

where m_e is the rest mass of the electron, x denotes the transverse coordinate perpendicular to the plane and γ means the Lorentz factor.

Since the crystal potential is periodic, the solutions of Eq. (1) are Bloch waves^{17,34}

$$\psi(x) = e^{ikx} \sum_n c_n e^{ingx} \quad (n = \dots, -1, 0, 1, 2, \dots) \quad (2)$$

where k is the electron wave vector and \vec{g} is the reciprocal lattice vector of the plane considered. The continuum potential expanded into a Fourier series reads

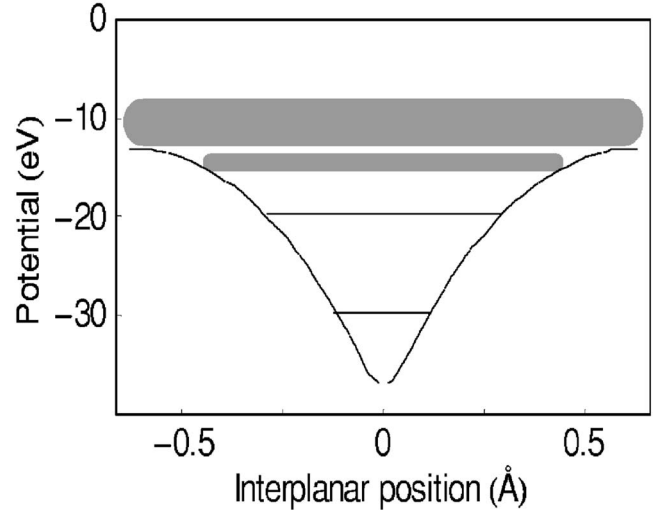


FIG. 1. Potential of the (110) plane of diamond and eigenvalues (bands) calculated for 17 MeV electron energy at a temperature of 300 K. Bound states are numbered upward by integers starting at the ground state with $n=0$.

$$V(x) = \sum_n v_n e^{ingx} \quad (n = \dots, -1, 0, 1, 2, \dots) \quad (3)$$

where v_n denote the Fourier coefficients of the periodic potential. Using the Doyle-Turner approach³⁵ for the electron-atom interaction they can be written as

$$v_n = -\frac{2\pi}{V_c} a_0^2 (e^2/a_0) \sum_j e^{-M_j(\vec{g})} e^{-i\vec{g} \cdot \vec{r}_j} \sum_{i=1}^4 a_i e^{[-1/4(b_i/4\pi^2)(ng)^2]}, \quad (4)$$

where V_c is the volume of unit cell, a_0 is the Bohr radius, e is the electron charge, \vec{r}_j represents the coordinates of the j atoms in the unit cell, a_i , b_i are tabulated coefficients,³⁵ and $M_j(\vec{g}) = \frac{1}{2} g^2 \langle u_j^2 \rangle$ denotes the Debye-Waller factor, which describes the thermal vibration of the j th atom with mean squared amplitude $\langle u_j^2 \rangle$.

The crystal structure of the diamond may be represented by an fcc lattice with a two-atom basis or, equivalently, by a cubic lattice with an eight-atom basis. Substitution of the expressions given above into Eq. (1) reduces the problem to the calculation of the eigenvalues of a matrix \mathbf{A} , which in the planar case consists of the components

$$A_{nm} = v_{n-m} \quad (n \neq m),$$

$$A_{nn} = \frac{\hbar^2}{2m\gamma} (k + ng)^2 + v_0. \quad (5)$$

For illustration, the shape of the potential of the (110) plane of diamond crystal is shown in Fig. 1, and the eigenvalues and Bloch bands calculated for an electron energy of 17 MeV³⁶ are indicated by horizontal lines and bars of different thickness, respectively. The probability densities of the three bound states relating to their squared wave functions are drawn in Fig. 2. Somewhat anticipating the consider-

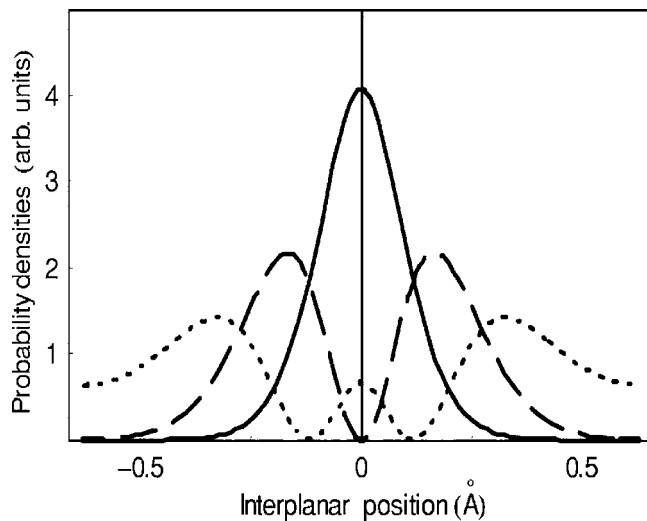


FIG. 2. Probability density distributions for electrons of energy 17 MeV channeled in the (110) plane of diamond (full line— $n=0$, dashed line— $n=1$, dotted line— $n=2$).

ations in the next section, we want to note that the abscissae of Figs. 1–3 are equally scaled to one interplanar distance.

The spontaneous transition of a channeled electron from a higher to a lower transverse state leads to the emission of a CR photon. Several mechanisms govern the formation of the residual line shape of CR and its linewidth as being registered by means of some spectrometer. In the following, we very briefly consider them in a somewhat phenomenological manner (i) to recapitulate the basic physics context and (ii) to relate them to the experimental conditions of CR production and measurement.

B. Coherence length

The intrinsic line shape of CR is connected with the finite lifetime of the channeling states. It is limited due to incoherent scattering of the channeled electrons, for diamond crystals mainly from phonons³⁷ (thermal scattering) but also from electrons of the crystal atoms.^{25,26,34,38,39} The resulting

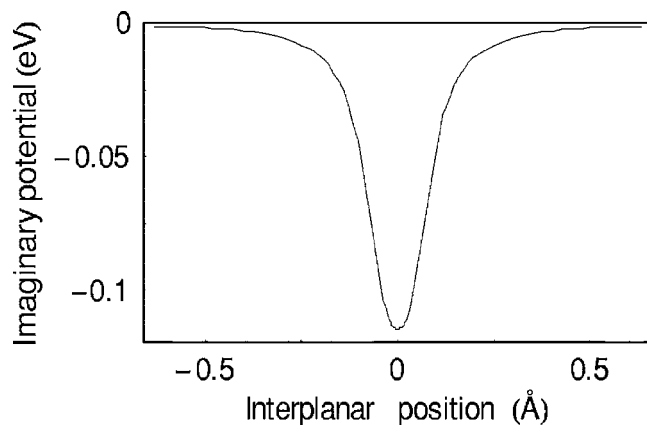


FIG. 3. Imaginary part of the potential of the (110) plane of diamond crystals for 17 MeV electron energy calculated at a temperature of 300 K.

CR line shape is a Lorentzian with a width given by

$$\Gamma_{coh} = \frac{2\gamma^2 \hbar c}{l}. \quad (6)$$

The total coherence length l is defined by

$$\frac{1}{l} = \frac{1}{l_1} + \frac{1}{l_2}, \quad (7)$$

where l_1 and l_2 are the coherence lengths of the initial and final state of some transition considered. In the framework of the theory of complex potential $U(x) = V(x) + iW(x)$, the coherence length reads

$$l_j = -\frac{\hbar \beta c}{2\langle W \rangle_j}, \quad (8)$$

where $\langle W \rangle_j = \langle \psi_j | W | \psi_j \rangle$ is the expectation value of the imaginary part of the complex potential for the state j and $\beta = \sqrt{\gamma^2 - 1} / \gamma$. Such as the real part $V(x)$ [cf. Eq. (3)], the imaginary part $W(x)$ can be expanded into a Fourier series

$$W(x) = \sum_n v_n^i e^{ingx} \quad (n = \dots, -1, 0, 1, 2, \dots), \quad (9)$$

where the Fourier coefficients read^{25,37}

$$v_g^i = \frac{\hbar^3 \beta N_V}{2m_0^2 c V_c} \int f_{el}(|\vec{q}|) f_{el}(|\vec{q} - \vec{g}|) \times [e^{-M_j(\vec{g})} - e^{-M_j(\vec{g}) - M_j(\vec{q} - \vec{g})}] q d q d \varphi, \quad (10)$$

$\vec{q} = \vec{k} - \vec{k}_0$ gives the change of the electron wave vector and $f_{el}(\vec{q})$ is the scattering amplitude.

Equation (10) can be reduced to²⁵

$$v_n^i = -\frac{\hbar^3 \pi N_V}{2m_0^2 c V_c} \sum_i \sum_j a_i a_j \left[\frac{e^{-M_j(\vec{g}) - B_i B_j n^2 g^2 / (B_i + B_j)}}{B_i + B_j} - \frac{e^{-C_i C_j n^2 g^2 / (C_i + C_j)}}{C_i + C_j} \right] \quad (11)$$

with $B_i = b_i / (16\pi^2)$ and $C_i = B_i + 0.5\langle u_i^2 \rangle$ using the Gaussian parametrization of the electron-scattering form factor,³⁵ $f_{el}(s)$, where $s = ng/4\pi$, N_V is the atomic density, and V_c is the volume of the unit cell. The expectation value, $\langle W \rangle_j$, therefore, describes the decay of a particular eigenstate due to incoherent scattering, where l_j gives the characteristic length for attenuation of the initial electron wave function. The lifetime of that channeling state is then $\tau_j = l_j / c$.

Note that the approximation of the electron-scattering form factor $f_{el}(s)$ using the parameters given by Doyle and Turner³⁵ is valid only for values of $s < 2 \text{ \AA}^{-1}$. When this is acceptable for a calculation of the eigenvalues, it leads to inaccurate coherence lengths, because incoherent scattering is effective at short distances from the channeling plane. This means that the Fourier components of $W(x)$ have to be evaluated at larger values of s . In our calculations of coherence lengths we, therefore, used the approximation of Ref. 25, which applies for $s \leq 6 \text{ \AA}^{-1}$ and leads to an increase of the calculated intrinsic linewidth by about (15–20)%. For illus-

TABLE I. Coherence lengths (μm) calculated for the two lowest transitions of (110) planar channeling radiation of diamond.

E_e (MeV)	1-0	2-1
14.6	1.11	3.21
17	1.06	2.91
30	0.90	1.99
34	0.87	1.86

tration, the imaginary part of the complex potential of the (110) plane of the diamond is shown in Fig. 3 for an electron energy of 17 MeV. It is weaker than the real continuum potential and more strongly located at the channeling plane.

The coherence lengths relating to the 1-0 and 2-1 transitions of (110) planar CR of the diamond have been calculated at four electron energies, E_e (Table I).

C. Finite crystal thickness

Another line broadening mechanism is connected with the finite thickness, z , of the crystal. This contribution relates to the life time of the channeling states. It reads^{25,26}

$$\Gamma_L = \frac{4\pi\gamma^2\hbar c}{z} \quad (12)$$

and can be neglected at larger z .

D. Bloch-wave broadening

It is inherent to the many-beam approach of channeling that the eigenvalues depend upon the electron wave vector k which can vary such as $0 \leq k \leq g/2$. This effect causes a band structure of the channeling states. The variation of the transverse energy with the electron wave vector is small for tightly bound states. For the states near the top of the potential well and within the continuum, however, this effect becomes the main line broadening mechanism.

At small observation angle, Bloch-wave line broadening is given by the sum of the band widths of the initial and the final state²⁵

$$\Gamma_{Bloch} = 2\gamma^2(|\varepsilon_i^{k=0} - \varepsilon_i^{k=g/2}| + |\varepsilon_f^{k=0} - \varepsilon_f^{k=g/2}|) \quad (13)$$

accurately speaking, by the band dispersions.

Apart from channeling inherent line broadening, the experimental conditions of CR production as well as measurement involve further components affecting the observed CR line shape.

E. Energy spread of the electron beam

The energy of a CR line, E_{CR} , scales with the electron energy such as

$$E_{CR} \propto \gamma^a, \quad (14)$$

where a is a constant ranging from 1.5 to 2 in dependence on the transition considered.¹⁷ Therefore, the initial beam-

energy spread, ΔE_e , causes an energy spread of the observed CR photons

$$\Delta E_{CR} = a \frac{\Delta E_e}{E_e}. \quad (15)$$

As at the ELBE beam, this contribution is usually negligible but exact beam-energy tuning is important.

F. Detector resolution

The often Gaussian-like response of the detector applied for CR spectrometry influences the observed CR line shape, which now represents a convolution of a Lorentzian with a Gaussian (Voigt profile).

G. Doppler broadening

Since the channeled electron is relativistic, the Lorentz transformation deepens the crystal potential by a factor γ . The dipole emission pattern of CR in the electron rest system transforms into an extremely forward directed cone, and due to the Doppler shift the CR energy observed at an angle ϑ with respect to the beam axis becomes

$$E_{CR} \cong \frac{2\gamma^2\hbar\omega}{1 + \gamma^2\vartheta^2}, \quad (16)$$

where the radiation frequency, ω , relates to the energy difference between the channeling states involved (cf., Fig. 1). Consequently, CR photons of maximum energy are emitted into direction $\vartheta=0$, and E_{CR} decreases with the observation angle. Note that CR covers the energy region of x rays at the beam energies considered in this work.

Concerning CR measurement, it directly follows from Eq. (16) that accurate adjustment of the detector position is important. The finite solid angle of the detector principally also influences the observed line shape but this effect is mostly negligible at typical measurement conditions. Otherwise, a large beam divergence can cause CR line broadening because the average observation angle becomes different from zero. In accordance with Eq. (16), line broadening is directed towards smaller energy, and the CR line shape becomes asymmetric.

H. Multiple scattering

Multiple small-angle scattering of the electrons in the crystal effectively affects the beam divergence at a depth z and, consequently, also excites line broadening and asymmetry. This broadening mechanism becomes relevant if thicker crystals are used.

Multiple scattering of electrons in amorphous materials (or randomly oriented crystals) is well understood. Its effect on the line shape of planar CR, i.e., when the channeled electron moves parallel to a crystal plane, is less investigated. The asymmetry of the line shape of planar CR of the diamond at electron energies of 54.2 and 80 MeV was first studied in Ref. 18, and CR spectra of Si could be interpreted by introducing some mean multiple-scattering angle in Ref.

19. The asymptotic behavior of CR spectra at large crystal thicknesses has been considered in Ref. 20.

The angular distribution of multiple scattering can be described by a Gaussian

$$f(\theta, z) = \frac{1}{\sqrt{2\pi}\theta_{ms}(z)} e^{-\theta^2/2\theta_{ms}^2(z)}. \quad (17)$$

The root-mean-squared (rms) multiple-scattering angle of electrons in amorphous media is given by⁴⁰

$$\Theta_{ms} = \left(\frac{14 \text{ MeV}}{E_e} \right) \sqrt{\frac{z}{L_0}} \left[1 + 0.038 \ln \left(\frac{z}{L_0} \right) \right], \quad (18)$$

where L_0 denotes the radiation length, and z is the thickness of the layer. For a randomly oriented diamond crystal the radiation length amounts to 12.23 cm.^{41,42} Note that L_0 means the path length in matter after which the electron energy was diminished by a factor of $1/e$ due to radiation losses.

The Doppler broadening of planar CR due to multiple scattering can be evaluated by²⁵

$$\Gamma_{Dopp} = \gamma^2 \Theta_{ms, ch}^2 E_{CR}. \quad (19)$$

Here $\Theta_{ms, ch}^2$ is an effective mean squared multiple-scattering angle relevant for the conditions of CR production and measurement.

To clarify the matter of investigation, let us depict the effect of multiple scattering classically. When scattering in the crystal spreads the incoming (low emittance) beam over a solid angle $\Delta\Omega_e(z; \phi, \theta)$, where ϕ denotes the azimuth with respect to the normal of the plane and θ means the scattering angle of the electron, planar channeling proceeds in the plane ($z; \phi = \frac{\pi}{2}, \theta$). Formally, there is no limit for θ but the observation angle of CR, ϑ , changes with θ . In accordance with Eq. (16), this causes a CR energy spread of $(-\gamma^2\vartheta^2)$. With Eq. (18) one can find that Θ_{ms} for thicker crystals becomes even larger than $1/\gamma$. On the other hand, dechanneling is connected with scattering components directed perpendicular to the channeling plane. Such components lead to intraband or interband scattering that governs the occupation dynamics due to migration of the channeled electrons to other states.

Equilibrium occupation of bound states is assumed to be reached after several micrometers of traveling through the crystal independent on the initial population.

Avoiding any assumptions about the scattering angle, θ , we tried to investigate the effect of multiple scattering on the line shape of planar CR relating to experimental data only. If a CR line in a measured spectrum is sufficiently well separated from lines resulting from other transitions, it is possible to determine the effective (rms) multiple-scattering angle, $\Theta_{ms, ch}(z)$, by fitting an appropriate asymmetric spectral distribution function to the observed line shape. The dependence of the ratio $\Theta_{ms, ch}/\Theta_{ms}$ on the crystal thickness will be investigated in the following sections.

I. Intensity

The differential transition rate of spontaneous planar CR per electron and per units of solid angle, photon energy and crystal thickness reads^{19,23,34,39}

$$\begin{aligned} \frac{d^3 N_{CR}(i \rightarrow f)}{d\Omega_x dE_x dz} &= \frac{e^2}{\pi m_e^2 c^4} \frac{E_x}{2\gamma^2(1 - \beta_{\parallel} \cos \vartheta)} \\ &\times \left[\sin^2 \varphi + \left[\frac{\cos \vartheta - \beta_{\parallel}}{1 - \beta_{\parallel} \cos \vartheta} \right]^2 \cos^2 \varphi \right] \\ &\left| \left\langle \psi_f \left| \frac{d}{dx} \right| \psi_i \right\rangle \right|^2 \delta \left[E_x - \frac{\varepsilon_i - \varepsilon_f}{1 - \beta_{\parallel} \cos \vartheta} \right] P_i(z), \quad (20) \end{aligned}$$

where $\langle \psi_f | \frac{d}{dx} | \psi_i \rangle$ is the transition matrix element, and $P_i(z)$ gives the occupation probability of the channeling state i as function of initial population and crystal thickness.

Taking into account a nonzero intrinsic CR linewidth, the δ function in Eq. (20) has to be substituted by a Lorentzian. Multiple scattering is involved by convolving the Lorentzian with a Gaussian given by Eq. (17). For CR registered within a narrow aperture $\Delta\vartheta \ll \gamma^{-1}$ at $\theta=0$ one can set $\vartheta \cong \theta$, and with the commonly used approximation

$$\frac{1}{1 - \beta_{\parallel} \cos \vartheta} \cong \frac{2\gamma^2}{1 + \gamma^2\vartheta^2}, \quad (21)$$

one finally obtains

$$\frac{d^2 N_{CR}(i \rightarrow f)}{d\Omega_x dE_x} = \frac{e^2}{\pi m_e^2 c^4} 2\gamma^2(\varepsilon_i - \varepsilon_f) \left| \left\langle \psi_f \left| \frac{d}{dx} \right| \psi_i \right\rangle \right|^2 \int_0^z dz P_i(z) \times \pi^{-3/2} \int_0^{+\infty} \frac{t^{-1/2} \Gamma_T(1 + 2\alpha^2 t) e^{-t}}{(E_x(1 + 2\alpha^2 t) - E_0)^2 + 0.25(1 + 2\alpha^2 t)^2 \Gamma_T^2} dt, \quad (22)$$

where the asymmetry parameter $\alpha = \gamma\theta_{ms, ch}$ accounts for the energy shift as well as for the broadening of the CR line due to multiple scattering, $E_0 = 2\gamma^2(\varepsilon_i - \varepsilon_f)$ means the maximum photon energy, and Γ_T is the Lorentzian linewidth. Note that the first integral in Eq. (22) refers to the population of the state i over a chosen crystal thickness z , and the second one

describes the shape of the registered CR line. With Eq. (17) one implies $\alpha = \alpha(z)$.

J. Linewidth

The calculation of the intensity of some CR line at given crystal thickness by means of Eq. (22) supposes that E_0, Γ_T ,

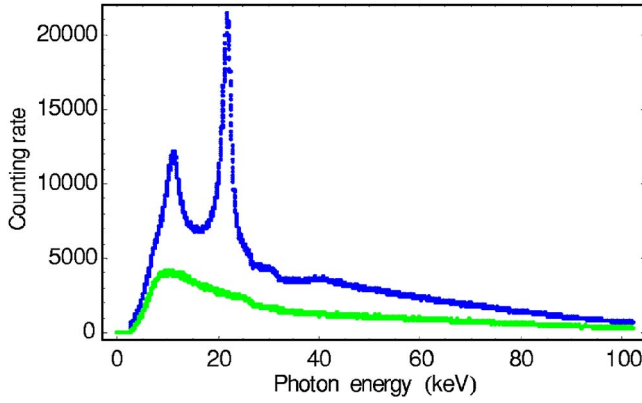


FIG. 4. (Color online) Spectra of (110) planar channeling radiation (upper one) and bremsstrahlung (lower one) measured for a 42.5 μm thick diamond crystal at the electron energy of 17 MeV.

$P_i(z)$, and $\alpha(z)$ are known. Within the scope of this work, we are interested in the evolution of the width of an observed CR line with increasing crystal thickness. Therefore, we want to omit any assumption about the occupation probability, $P_i(z)$, and to prove $\alpha(z)$ by fitting a spectral distribution of the form^{18,25}

$$P(E_x)dE_x = \pi^{-3/2}dE_x \times \int_0^{+\infty} \frac{t^{-1/2}\Gamma_T(1+2\alpha^2t)e^{-t}}{(E_x(1+2\alpha^2t)-E_0)^2+0.25(1+2\alpha^2t)^2\Gamma_T^2} dt \quad (23)$$

to the measured CR lines. At fixed γ and crystal thickness, z , this procedure provides values for the parameters α , E_0 , and Γ_T , respectively. Note that the fit parameter, Γ_T , in Eq. (23) incorporates small components of Bloch-wave broadening as well as the detector resolution. Therefore, as already mentioned in Ref. 23, the residual width of an observed CR line, Γ , cannot be simply determined neither by linear nor by quadratic summation of the partial contributions. Indeed, when the widths of two convolved Lorentzians add linearly, those of two Gaussians add quadratic, and the width of a Voigt profile has no adequate analytical expression and can be given only approximately. The sometimes used estimation^{21,25}

$$\Gamma^2 = \Gamma_{coh}^2 + \Gamma_L^2 + \Gamma_{Bloch}^2 + \Gamma_{det}^2 + \Gamma_{beam}^2 + \Gamma_{Dopp}^2 \quad (24)$$

ignores these circumstances.

IV. SPECTRUM ANALYSIS

The procedure of data reduction includes the following steps.²⁸ First, the spectra of CR and bremsstrahlung (BS), measured at aligned and random orientation of the diamond crystal, respectively, have to be normalized to the same number of incident electrons using the SEM monitor data. Subsequently, the normalized spectra have to be corrected for registration efficiency, self-absorption of radiation in the crystal and attenuation in window materials on the path from the target to the detector. Exemplarily, raw data spectra of (110) planar CR and BS registered for a diamond crystal of

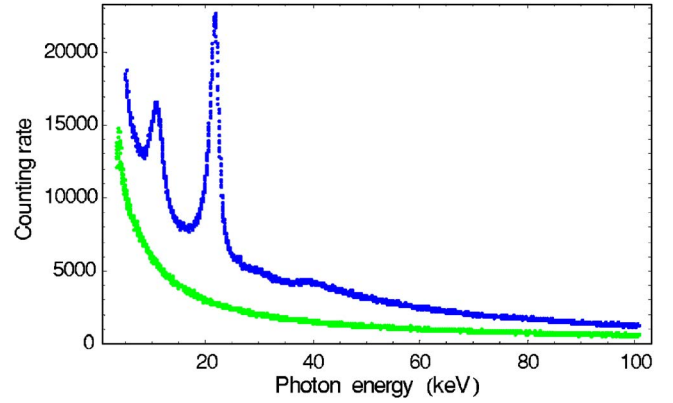


FIG. 5. (Color online) Spectra of (110) planar channeling radiation (upper one) and bremsstrahlung (lower one) as shown in Fig. 4 but corrected for registration efficiency, self-absorption and attenuation.

thickness 42.5 μm at an electron energy of 17 MeV are shown in Fig. 4. The result of this correction procedure is shown in Fig. 5.

After subtraction of the BS background, the CR spectrum consists of CR peaks (arising in the example shown in Fig. 5 from the two possible transitions 1-0 and 2-1) and remaining background components, e.g., from so-called free-to-bound transitions.

A least-squares curve fit has now been performed applying the Levenberg-Marquardt method for minimization of the χ^2 function. The CR peaks are approximated by a spectral distribution defined by Eq. (23), additional quasifree peaks are modeled by Gaussians, and a low-order polynomial accounts for the remaining background components. The energies of the CR lines calculated by means of the many-beam method were used as starting parameters for the fitting procedure.³⁶

The CR line shapes as obtained from the fitting procedure are shown in Fig. 6 for three transitions of (110) planar CR registered for a 168 μm thick diamond crystal at the electron energy of 30 MeV.

In order to examine the influence of multiple scattering on the line shapes, we also fitted Voigt profiles to our experimental data. For illustration, the background corrected spec-

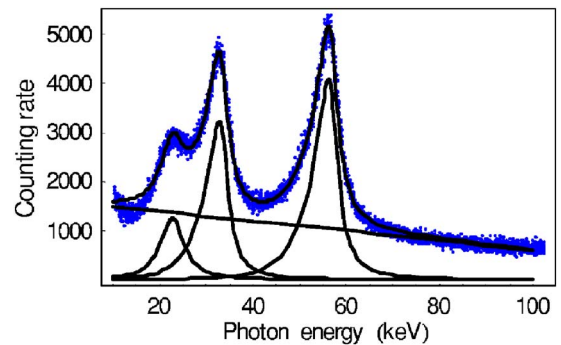


FIG. 6. (Color online) Line shapes of three transitions of (110) planar channeling radiation registered for a 168 μm thick diamond crystal at the electron energy of 30 MeV.

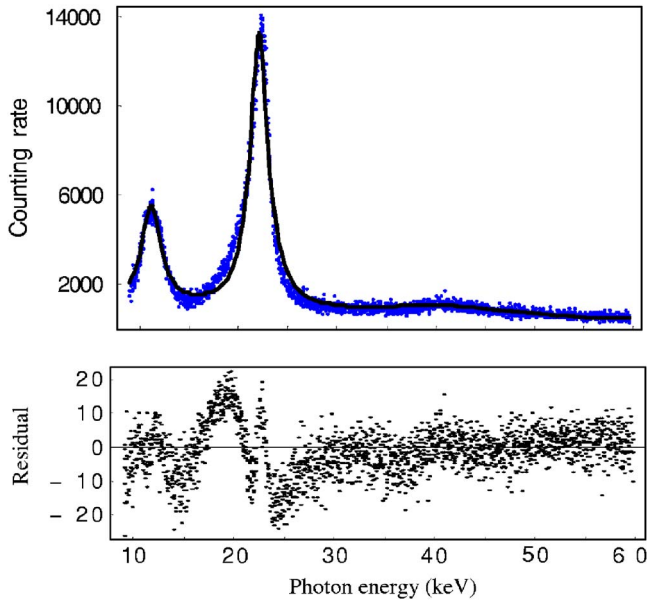


FIG. 7. (Color online) Measured spectral distribution of (110) planar channeling radiation for a 168 μm thick diamond crystal at the electron energy of 17 MeV and two Voigt profiles fitted to the CR lines. The lower part shows the residuals between the measured and the approximated line shapes.

trum of (110) planar CR registered for a 168 μm thick diamond crystal at the electron energy of 17 MeV is shown in Fig. 7 together with two approximated Voigt profiles, and in Fig. 8 with two asymmetric profiles given by Eq. (23).

To compare the quality of these two approximations of the CR line shape, the weighted deviations between the measured and modeled spectral distributions (residuals) are

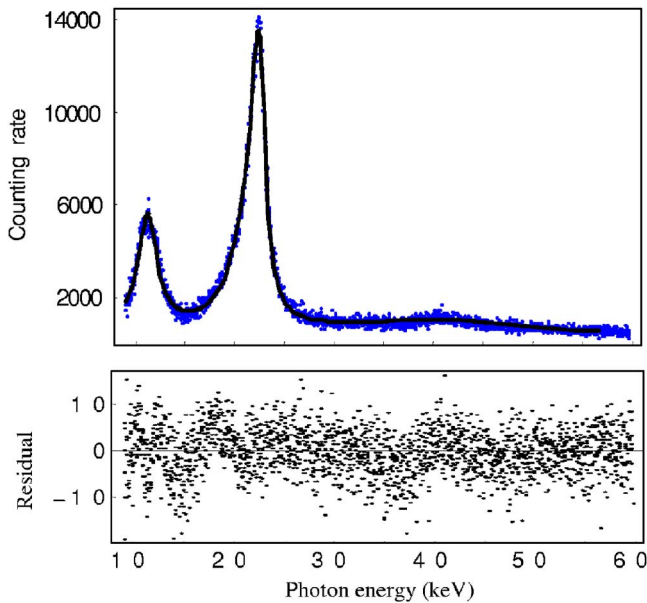


FIG. 8. (Color online) Measured spectral distribution of (110) planar channeling radiation for a 168 μm thick diamond crystal at the electron energy of 17 MeV and two asymmetric profiles given by Eq. (23). The lower part shows the residuals between the measured and the approximated line shapes.

TABLE II. Asymmetry parameters and mean multiple-scattering angles as obtained by fitting of asymmetric profiles given by Eq. (23) to the line shapes measured for the 1-0 transition of (110) planar channeling radiation of diamond. Column 4 lists the ratio to the values calculated by Eq. (18).

E_e (MeV)	α	$\Theta_{ms,ch}$ (mrad)	$\Theta_{ms,ch}/\Theta_{ms}$
42.5 μm			
14.6	0.172	6.03	0.55
17	0.177	5.32	0.56
30	0.168	2.87	0.54
34	0.175	2.60	0.56
102 μm			
17	0.211	6.33	0.41
30	0.216	3.69	0.42
168 μm			
14.6	0.246	8.62	0.36
17	0.230	6.91	0.33
30	0.226	3.84	0.33
500 μm			
14.6	0.278	9.73	0.22
17	0.281	8.46	0.22
30	0.311	5.31	0.24

shown in the lower parts of Figs. 7 and 8 respectively. Systematic deviations of the residuals from zero observed in the lower part of Fig. 7 near the position of the prominent peak certify a remarkable asymmetry of this CR line. Although this fact can inherently be seen in the measured spectrum (because this example has been especially chosen to demonstrate the procedure), in such cases, when the asymmetry is smaller, visual inspection can easily fail. Even formal proofing of the value of χ^2 resulting from the fitting procedure can lead to inadequate conclusions because the fit parameters involved are correlating variables. The residuals shown in the lower part of Fig. 8, however, are spread uniformly around zero providing confidence in the resulting values of the fit parameters.

V. RESULTS

The values for the asymmetry parameter obtained from the analysis of our measurements are presented in Table II.

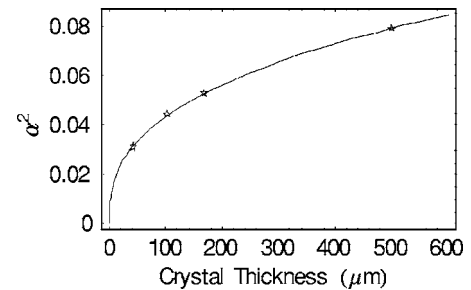


FIG. 9. Squared asymmetry parameter as obtained for the electron energy of 17 MeV drawn versus the crystal thickness.

TABLE III. Partial widths contributing to the residual linewidth as evaluated by means of Eq. (24) for the 1-0 transition of (110) planar channeling radiation for a diamond crystal of thickness 42.5 μm .

E_e (MeV)	Γ_{coh} (keV)	Γ_{Bloch} (keV)	Γ_{Dopp} (keV)	Γ_{det} (keV)	Γ_{calc} (keV)
14.6	0.29	0.26	0.50	0.47	0.87
17	0.41	0.17	0.69	0.49	0.95
30	1.51	0.02	1.61	0.60	2.29
34	2.01	0.01	2.15	0.63	3.01

The effective (rms) multiple-scattering angles for the 1-0 transition are listed in column 3 of Table II. The mean multiple-scattering angles as calculated by means of Eq. (18), and the accordant ratios $\Theta_{ms, ch}/\Theta_{ms}$ are given in column 4 of Table II.

From Table II one can conclude that the asymmetry parameter does not significantly change with the electron energy for each crystal thickness considered. The slightly higher value at the crystal thickness of 500 μm at 30 MeV can be understood because there one observes a small overlap of the CR peaks resulting from the transitions 1-0 and 2-1. Consequently, the dependence $\Theta_{ms, ch} \sim 1/E_e$ holds as given in Eq. (18).

For the illustration, Fig. 9 shows the values obtained for the squared asymmetry parameter at the electron energy of 17 MeV drawn versus the crystal thickness. It is obvious that the dependence on the crystal thickness is not linear as one would expect from Eq. (18) but can be described by a function of the form $\alpha^2 = sL^b$ where the coefficient s merges the ordinate scale and the exponent $b=0.37$. This means that the multiple-scattering angle effective for CR observation increases more slowly with the crystal thickness than given by Eq. (18). The ratio $\Theta_{ms, ch}/\Theta_{ms}$ is listed in column 3 of Table II.

Note that $\Theta_{ms, ch}$ is 1.5-4 times larger than the critical angle⁴³ for channeling along the (110) plane of the diamond at all energies considered. As expected, line broadening and energy shift is connected with in-plane scattering only. Furthermore, the values found for $\Theta_{ms, ch}$ are much less than $1/\gamma$.

The contributions to the residual linewidth, Γ , as calculated in accordance with Sec. III are listed in Table III for the crystal thickness of 42.5 μm . The partial widths due to Doppler broadening are calculated by means of Eq. (19) with the values for $\Theta_{ms, ch}$ given in Table II. The linewidth evaluated by means of Eq. (24), Γ_{calc} , is given in column 6 of Table III.

Table IV lists the CR peak energies obtained from the fitted profiles, E_{exp} , and the calculated transition energies, E_{calc} . Column 4 of Table IV clarifies that the peak-energy shift caused by multiple scattering, δE , increases with the crystal thickness at given electron energy, but it also increases with the electron energy at given thickness. The latter effect is connected with the dependence $E_0 \sim \gamma^2$ while the asymmetry parameter, α does not depend on γ (cf., Table II). Then the relative energy shift, $\delta E/E_0$, should not vary with the electron energy²⁵ (cf., column 5 of Table IV). This means that the peak-energy shift behaves such as $\delta E \sim \gamma^2$.

The residual linewidths (FWHM) of the approximated asymmetric profiles, Γ_{exp} , and the values found for Γ_T are

TABLE IV. Measured and calculated energies for the 1-0 transition of (110) planar channeling radiation of diamond. Since these values are congenersly afflicted with uncertainties and possible systematic deviations, errors are not given.

L (μm)	E_{exp} (keV)	E_0 (keV)	δE (keV)	$\delta E/E_0$	E_{calc} (keV)
14.6 MeV					
42.5	16.58	16.76	0.18	0.011	17.06
168	16.99	17.21	0.22	0.013	
500	16.47	16.75	0.28	0.017	
17 MeV					
42.5	21.72	21.96	0.24	0.011	22.23
102	21.42	21.70	0.28	0.012	
168	22.37	22.65	0.28	0.012	
500	21.38	21.68	0.30	0.014	
30 MeV					
42.5	56.19	56.87	0.68	0.012	59.49
102	56.72	57.71	0.99	0.017	
168	56.22	57.00	0.78	0.014	
500	55.06	56.61	1.55	0.027	
34 MeV					
42.5	70.02	70.96	0.94	0.013	73.78

TABLE V. Measured and calculated linewidths for the 1-0 transition of (110) planar channeling radiation of the diamond.

L (μm)	Γ_{exp} (keV)	Γ_T (keV)	Γ_{Dopp} (keV)	Γ_{calc} (keV)
14.6 MeV				
42.5	1.51	1.09	0.50	0.87
168	1.80	1.07	1.02	1.25
500	2.20	1.31	1.30	1.48
17 MeV				
42.5	2.00	1.45	0.69	0.95
102	2.19	1.45	0.98	1.18
168	2.47	1.44	1.16	1.39
500	2.77	1.26	1.74	1.90
30 MeV				
42.5	5.88	4.25	1.61	2.29
102	7.94	5.75	2.67	3.13
168	6.12	3.94	2.89	3.32
500	11.98	7.99	5.53	5.77
34 MeV				
42.5	7.84	6.00	2.15	3.01

listed in Table V together with the widths estimated by means of Eq. (24), Γ_{calc} . As an effect of multiple scattering, the linewidth considerably increases with the crystal thickness at given electron energy, while Γ_T is found to be rather constant. This behavior is expected, if the leading term of Γ_T is that given by Eq. (6). The increase of Γ_T with energy is for given thickness more pronounced than that of Γ_{Dopp} . The experimental linewidths are larger than the estimated ones because Eq. (24) underestimates the width of the convolution in Eq. (23). Otherwise, Γ_{exp} is slightly smaller than the sum $\Gamma_T + \Gamma_{Dopp}$.

After a small correction for Bloch-wave broadening and detector resolution, the values obtained from the fitting procedure for Γ_T (Table V) allows some estimation of the coherence length by means of Eq. (6). Table VI gives a comparison of calculated and experimentally found coherence lengths, where we adjoined the data of Ref. 23 obtained at electron energies of 5.2 and 9 MeV and those of Ref. 18 obtained at 53.2 and 80.3 MeV. From columns 3 and 4 of

Table VI one can conclude that the coherence length relating to the 1-0 transition of (110) planar CR for diamond crystals is nearly independent on the electron energy.^{18,23} In average it amounts to $(0.64 \pm 0.04) \mu\text{m}$.

Following the arguments of Ref. 18 that thermal scattering is not localized, we find a mean value of $(1.28 \pm 0.02) \mu\text{m}$ for the coherence length of the two most tightly bound channeling states in the (110) plane of the diamond at room temperature.

Comparison of columns 2 and 4 of Table VI reveals that the coherence lengths calculated by means of the optical potential method are about 1.5 times larger than the observed ones. Although in the diamond thermal scattering dominates, incoherent scattering of channeled electrons occupying tightly bound states on the electrons of the crystal atoms should also contribute. According to Ref. 26, the relation between these two scattering mechanisms is round about 4:1 at 54 MeV, and it should slightly decrease with decreasing energy.

VI. CONCLUSIONS

Measurements of planar CR have been carried out at electron energies of 14.6, 17, 30, and 34 MeV using diamond crystals of thickness between 42.5 and 500 μm .

The analysis of different line-broadening mechanisms contributing to the residual width of the CR line registered from the 1-0 transition of (110) planar channeling shows that with increasing crystal thickness multiple scattering increasingly affects the spectral line shape. For the first time, the influence of in-plane multiple scattering on planar CR has been investigated systematically at relatively large variation of the crystal thickness and the electron energy as well.

The method of fitting a convolution of a Lorentzian-like intrinsic line shape with a Gaussian-like distribution of the multiple-scattering angle to the measured spectral lines of CR provides a consistent picture about the additional line broadening as well as the peak-energy shift due to multiple scattering. It could be shown that the ratio of the mean multiple-scattering angle effective for planar CR observation in forward direction to that calculated for an amorphous target, $\Theta_{ms,ch}/\Theta_{ms}$, decreases with increasing crystal thickness and does not depend on the electron energy. If $\Theta_{ms,ch}$ de-

TABLE VI. Coherence lengths for the 1-0 transition of (110) planar channeling radiation of the diamond as calculated by means of the optical potential method, l_{calc} , as given in Refs. 18 and 23, l_{ref} , and as found from our measurements for crystals thicknesses of 42.5, 102, 168, and 500 μm .

E (MeV)	l_{calc} (μm)	l_{ref} (μm)	$l_{42.5}$ (μm)	l_{102} (μm)	l_{168} (μm)	l_{500} (μm)
5.2		0.64				
9.0		0.68				
14.6	1.11		0.68		0.69	0.54
17	1.06		0.66	0.65	0.65	0.76
30	0.90		0.65	0.48	0.70	0.34
34	0.87		0.59			
53.2		0.59				
80.3		0.62				

pend in the same manner on the electron energy such as for an amorphous target, the underlying scattering mechanism seems to be the same in both cases. With increasing crystal thickness it should, however, become less probable that scattered electrons remain in channeling condition because of the limited occupation length. Therefore, the mean multiple-scattering angle which is effective for the observed line shape of CR is smaller than that calculated by means of Eq. (18).

One should notice that the formal application of Eq. (18) in Ref. 19 allowed a satisfactory interpretation of measured spectra of planar CR for silicon, however, the crystal thickness amounted to only 10–20 μm . The results of the present work do not confirm those found earlier in Ref. 18 where (at that time) a somewhat simplified method had to be applied because the measured spectra were rather complex. The statement $\Theta_{ms, ch} = 0.3 \times \Theta_{ms}$ made in Ref. 25 should not have general validity.

The asymptotic behavior of channeled electrons in thick crystals has been investigated theoretically in Ref. 20. The calculation of CR spectra, however, needed in several assumptions where that of uniform line broadening makes the principal difference to our approach. As has been shown in our analysis, multiple scattering causes a remarkable line broadening and a small peak-energy shift as well. This means that the residual width of a planar CR line depends on the multiple-scattering angle what is ignored in Eq. (5) of Ref. 20. Since comparison of calculated spectra with measured ones has been made at the rather high electron energy

of 54 MeV, the intrinsic line width dominates and the effect of multiple scattering becomes relatively smaller.

As expected, the residual linewidth of planar CR cannot be explained neither by a linear²⁶ nor by a quadratic²¹ additive of the partial contributions to line broadening because it results from the convolution of different distribution functions. This basic idea expressed in Ref. 18 and further developed in Refs. 19 and 25 has been consequentially applied for data reduction in this work because the CR line shapes observed in our measurements show a remarkable degree of asymmetry. Note that Eq. (4.64) of Ref. 25 is adequate to Eq. (23) except a misprint in the exponential function where the variable $-x$ must be changed to $-x^2$.

Planar CR line broadening due to multiple scattering is of the order of 1–2 keV even for a relatively large thickness of the diamond crystal. Compared with broadening, the peak-energy shift is much less. Concerning a possible application of CR as a quasimonochromatic x-ray source, this fact turns to be a precondition for the use of thicker crystals.^{24,28} Within the scope of this paper, we knowingly omit considerations about the intensity of planar CR because this will be the topic of a forthcoming work. Since our method automatically provides realistic approximations for the intrinsic linewidth of CR, coherence lengths relating to the considered CR transition have been deduced and were found to be in good agreement with earlier results of Refs. 18 and 23. This supports the conclusion that the coherence length of tightly bound channeling states is insensitive to the electron energy.

*On leave from School of Sciences, Tarbiat Moallem University of Sabzevar, Iran.

†Corresponding author, w.wagner@fz-rossendorf.de, phone +49 351 260 23 54, fax +49 351 260 37 00.

¹M. A. Kumakhov, Phys. Lett. **57**, 17 (1976).

²J. U. Andersen, A. K. Andersen, and W. M. Augustyniak, K. Dan. Vidensk. Selsk. Mat. Fys. Medd. **39**, 10 (1977).

³R. W. Terhune and R. W. Pantell, Appl. Phys. Lett. **30**, 265 (1977).

⁴V. G. Baryshewsky and I. Ya. Dubovskaya, Phys. Status Solidi B **82**, 403 (1977).

⁵A. W. Sáenz and H. Überall, *Coherent Radiation Sources* (Springer, Heidelberg, 1985).

⁶R. A. Carrigan and J. A. Ellison, *NATO Advanced Research Workshop on Relativistic Channeling* (Plenum, New York-London, 1987).

⁷M. A. Kumakhov and F. F. Komarov, *Radiation from Charged Particles in Solids* (AIP, New York, 1989).

⁸M. A. Kumakhov and R. Wedell, *Radiation of Relativistic Light Particles During Interaction with Single Crystals* (Spektrum Akademischer Verlag, Heidelberg, 1991).

⁹A. I. Akhiezer and N. F. Shul'ga, *High-Energy Electrodynamics in Matter* (Gordon and Breach Sci. Publ., Amsterdam, 1996).

¹⁰P. Rullhusen, X. Artru, and P. Dhez, *Novel Radiation Sources Using Relativistic Electrons* (World Scientific, Singapore, 1998).

¹¹H. Genz, H.-D. Gräf, P. Hoffmann, W. Lotz, U. Nething, A. Rich-

ter, H. Kohl, A. Weickenmeier, W. Knüpfer, and J. P. F. Sell-schop, Appl. Phys. Lett. **57**, 2956 (1990).

¹²C. K. Gary, R. H. Pantell, M. Özcan, M. A. Piestrup, and D. G. Boyers, J. Appl. Phys. **70**, 2995 (1991).

¹³A. Richter, Mater. Sci. Eng., B **11**, 139 (1992).

¹⁴A. Richter, in *Proceedings Fifth EPAC*, edited by S. Myers *et al.* (IOP Publishing, Bristol, 1996); <http://linaxa.ikp.physik.tu-darmstadt.de/richter/s-dalinac/>, January 20, 2006.

¹⁵Radiation Source ELBE, <http://www.fz-rossendorf.de/>, January 20, 2006.

¹⁶M. Gouanere, D. Sillou, M. Spighel, N. Cue, M. J. Gaillard, R. G. Kirsch, J.-C. Poizat, J. Remillieux, B. L. Berman, P. Catillon, L. Roussel, and G. M. Temmer, Nucl. Instrum. Methods Phys. Res. **194**, 225 (1982).

¹⁷R. K. Klein, J. O. Kephart, R. H. Pantell, H. Park, B. L. Berman, R. L. Swent, S. Datz, and R. W. Fearick, Phys. Rev. B **31**, 68 (1985).

¹⁸M. Gouanere, D. Sillou, M. Spighel, N. Cue, M. J. Gaillard, R. G. Kirsch, J.-C. Poizat, J. Remillieux, B. L. Berman, P. Catillon, L. Roussel, and G. M. Temmer, Phys. Rev. B **38**, 4352 (1988).

¹⁹J. O. Kephart, B. L. Berman, R. H. Pantell, S. Datz, R. K. Klein, and H. Park, Phys. Rev. B **44**, 1992 (1991).

²⁰L. I. Ognev, Nucl. Instrum. Methods Phys. Res. B **84**, 319 (1994).

²¹U. Nething, Ph.D. thesis, Technische Hochschule Darmstadt, 1994.

- ²²U. Nething, M. Galemann, H. Genz, M. Höfer, P. Hoffmann-Staschek, J. Hormes, A. Richter, and J. P. F. Sellschop, *Phys. Rev. Lett.* **72**, 2411 (1994).
- ²³H. Genz, L. Groening, P. Hoffmann-Staschek, A. Richter, M. Höfer, J. Hormes, U. Nething, J. P. F. Sellschop, C. Toepffer, and M. Weber, *Phys. Rev. B* **53**, 8922 (1996).
- ²⁴I. Reiz, Diploma thesis, TU Darmstadt, 1999 (unpublished); H. Genz, in *Electron-Photon Interaction in Dense Media, Proceedings NATO Advanced Research Workshop on Electron-Photon Interaction in Dense Media, Nor-Hamberd, Yerevan, Armenia, 2001*, edited by H. Wiedemann, NATO Science Series II, Vol. 49, p. 217 (Kluwer Acad. Publ., Dordrecht, 2002).
- ²⁵K. Chouffani and H. Überall, *Phys. Status Solidi B* **213**, 107 (1999).
- ²⁶A. F. Burenkov, Yu. I. Dudchik, and F. F. Komarov, *Radiat. Eff.* **83**, 241 (1984).
- ²⁷W. Wagner, A. Panteleeva, J. Pawelke, and W. Enghardt, *Wiss.-Tech. Ber. - Forschungszent. Rossendorf* **401**, 56 (2004).
- ²⁸W. Wagner, B. Azadegan, A. Panteleeva, J. Pawelke, and W. Enghardt, in *Proceedings International Conference on Charged and Neutral Particles Channeling Phenomena, Frascati, Italy, 2004*, edited by S. B. Dabagov (SPIE, Bellingham, 2005), Vol. 5974.
- ²⁹W. Wagner, B. Azadegan, J. Pawelke, and W. Enghardt, *Wiss.-Tech. Ber. - Forschungszent. Rossendorf* **423**, 69 (2005).
- ³⁰W. Wagner, F. Müller, A. Nowack, M. Sobiella, J. Steiner, and W. Enghardt, *Wiss.-Tech. Ber. - Forschungszent. Rossendorf* **423**, 72 (2005).
- ³¹W. Neubert, K. Heidel, J. Hutsch, M. Langer, and K.-H. Herrmann, *Wiss.-Tech. Ber. - Forschungszent. Rossendorf* **341**, 16 (2002).
- ³²W. Neubert, K. Heidel, J. Pawelke, W. Wagner, and W. Enghardt, *Wiss.-Tech. Ber. - Forschungszent. Rossendorf* **423**, 73 (2005).
- ³³W. Neubert, J. Pawelke, W. Wagner, and W. Enghardt, *Wiss.-Tech. Ber. - Forschungszent. Rossendorf* **423**, 74 (2005).
- ³⁴J. U. Andersen, E. Bonderup, E. Lægsgaard, and A. H. Sørensen, *Phys. Scr.* **28**, 308 (1983).
- ³⁵P. A. Doyle and P. S. Turner, *Acta Crystallogr., Sect. A: Cryst. Phys., Diffr., Theor. Gen. Crystallogr.* **24**, 390 (1968).
- ³⁶B. Azadegan, L. Sh. Grigoryan, J. Pawelke, and W. Wagner, *Wiss.-Tech. Ber. - Forschungszent. Rossendorf* **423**, 68 (2005).
- ³⁷G. Radi, *Acta Crystallogr., Sect. A: Cryst. Phys., Diffr., Theor. Gen. Crystallogr.* **26**, 41 (1970); M. J. Whelan, *J. Appl. Phys.* **36**, 2103 (1965).
- ³⁸D. M. Bird and B. F. Buxton, *Proc. R. Soc. London, Ser. A* **379**, 459 (1982).
- ³⁹M. Weber, Ph.D. thesis, University of Erlangen, 1995.
- ⁴⁰V. L. Highland, *Nucl. Instrum. Methods* **129**, 497 (1975); **161**, 171 (1979).
- ⁴¹Y. S. Tsai, *Rev. Mod. Phys.* **46**, 815 (1974).
- ⁴²S. Eidelman *et al.*, *Phys. Lett. B* **592**, 246 (2004).
- ⁴³J. Lindhard, *Phys. Lett.* **12**, 126 (1964).